

Single-spin asymmetries in inclusive deep inelastic scattering and multiparton correlations in the nucleon

A. Metz¹, D. Pitonyak¹, A. Schäfer², M. Schlegel³, W. Vogelsang³, J. Zhou²

¹*Department of Physics, Barton Hall, Temple University, Philadelphia, PA 19122, USA*

²*Institute for Theoretical Physics, Regensburg University,
Universitätsstraße 31, D-93053 Regensburg, Germany*

³*Institute for Theoretical Physics, Tübingen University,
Auf der Morgenstelle 14, D-72076 Tübingen, Germany*

April 1, 2021

Abstract

Transverse single-spin asymmetries in inclusive deep inelastic lepton-nucleon scattering can be generated through multiphoton exchange between the leptonic and the hadronic part of the process. Here we consider the two-photon exchange and mainly focus on the transverse target spin asymmetry. In particular, we investigate the case where two photons couple to different quarks. Such a contribution involves a quark-photon-quark correlator in the nucleon, which has a (model-dependent) relation to the Efremov-Teryaev-Qiu-Sterman quark-gluon-quark correlator T_F . Using different parametrizations for T_F we compute the transverse target spin asymmetries for both a proton and a neutron target and compare the results to recent experimental data. In addition, potential implications for our general understanding of single-spin asymmetries in hard scattering processes are discussed.

1 Introduction

In order to describe deep inelastic lepton-nucleon scattering (DIS), $\ell(k) + N(P) \rightarrow \ell(k') + X$, one normally considers the exchange of only one photon between the leptonic and the hadronic part of the process¹. In this one-photon exchange approximation, the cross section for DIS can be expressed in terms of four structure functions: two for unpolarized scattering and two for double-polarized scattering where both beam and target are polarized. On the other hand, because of parity and time reversal invariance, single-spin observables are forbidden in the one-photon exchange approximation [1]. However, this restriction does not apply if a multiphoton exchange is taken into account. In this case there can be a nonzero single-spin effect due to a correlation of the type

$$\varepsilon^{SPkk'} \equiv \varepsilon_{\mu\nu\rho\sigma} S^\mu P^\nu k^\rho k'^\sigma, \quad (1)$$

where $\varepsilon^{\mu\nu\rho\sigma}$ is the totally antisymmetric Levi-Civita tensor. The four-vector S may represent the spin-vector of the nucleon, the incoming lepton, or the outgoing lepton. The correlation in Eq. (1) is nonzero provided that S has a component which is normal to the reaction plane. Therefore, one can

¹Throughout this work we neglect contributions from the Z-boson exchange.

have a transverse single-spin asymmetry (SSA) defined through

$$A_{UT} = \frac{d\sigma^\uparrow - d\sigma^\downarrow}{d\sigma^\uparrow + d\sigma^\downarrow} = \frac{d\sigma^\uparrow - d\sigma^\downarrow}{2 d\sigma_{unp}}, \quad (2)$$

where the numerator is given by the difference of the cross sections when the nucleon's (transverse) spin vector is flipped. (Note that the corresponding transverse SSA in the case of, e.g., $p^\uparrow p \rightarrow \pi X$ is often denoted by A_N .) A precise definition of our sign conventions for A_{UT} is given below. The asymmetry A_{UT} can be expected to be small for it is proportional to the electromagnetic fine structure constant $\alpha_{em} \approx 1/137$.

While for elastic lepton-nucleon scattering multiphoton exchange has already been extensively studied — see [2, 3] and references therein, our knowledge about multiphoton exchange in DIS is still rather limited, in particular when it comes to the spin asymmetry A_{UT} . Early measurements of A_{UT}^p (asymmetry for a polarized proton) were performed at the Cambridge Electron Accelerator [4] and at the Stanford Linear Accelerator [5]. These experiments were carried out in the resonance region, and in either case the asymmetry was found to be zero within the error bars. The recent measurement of A_{UT}^p by the HERMES Collaboration [6] constitutes the first such study in the DIS region. Both an electron and a positron beam were used, and again no evidence for a nonzero effect was found [6]. Moreover, by using a polarized ^3He target, preliminary data on A_{UT}^n (asymmetry for a polarized neutron) were obtained in the E07-013 experiment in Hall A at Jefferson Lab [7, 8], providing for the first time a nonvanishing transverse SSA in DIS on the (few) percent level. The challenging task is to describe both the magnitude and the sign of the proton and neutron data.

On the theoretical side there exists an early phenomenological calculation of A_{UT}^p which concentrates on the nucleon-pion final state, in a kinematical region where the reaction is dominated by the excitation and the decay of the $\Delta(1232)$ resonance [9]. More recently an attempt was made to describe transverse SSAs in inclusive DIS in the parton model [10]. That work considered the coupling of the exchanged photons to the *same* quark inside the nucleon. While a compact and well-behaved result for the beam spin asymmetry was obtained, the transverse target SSA turned out to be infrared (IR) divergent [10]. We review these results below in Sec. 2 and explain how the IR divergence can be removed. If one keeps quark mass effects, the target SSA also receives a contribution involving the transversity distribution of the nucleon [11]. An estimate of this effect gave rise to quite small results for both A_{UT}^p and A_{UT}^n [11]. We also point out that in Ref. [12] the influence of two-photon exchange on observables in semi-inclusive DIS has been explored for the first time.

In the present work we mainly focus on the situation when the exchanged photons couple to *different* quarks inside the nucleon. As we are going to argue below, numerically this contribution presumably dominates over the one where the photons couple to the same quark. The required collinear twist-3 calculation is very similar to the treatment of transverse SSAs in hadron-hadron scattering [13–17]. The analytical result for the target asymmetry depends on a quark-photon-quark correlator ($q\gamma q$ -correlator). By using a valence quark picture of the nucleon, we relate this object to the so-called Efremov-Teryaev-Qiu-Sterman (ETQS) quark-gluon-quark correlator (qgq -correlator) T_F [13–15], which plays an important role in the quantum chromodynamics (QCD) description of SSAs. On the basis of different parametrizations for T_F , we then compute A_{UT}^p and A_{UT}^n . Depending on the input for T_F this approach does provide a reasonable description of the available data. Our finding also has potential implications for the general understanding of single-spin asymmetries in hard scattering processes.

The paper is organized as follows: in Sec. 2 we consider the two-photon exchange where both photons couple to the same quark. In that part we briefly review what is already known from the literature [10, 11], but also provide some new insights. Section 3 then deals with the coupling of the two photons to different quarks. There we provide the analytical result for the transverse target SSA,

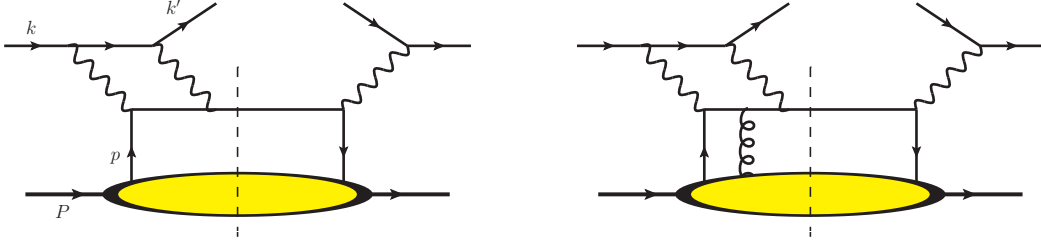


Figure 1: Left panel: Two-photon exchange contribution (box graph) to inclusive DIS in the parton model. The Hermitian conjugate diagram, not shown in the figure, has to be considered as well. The so-called crossed box graph does not contribute to A_{UT} . Right panel: Sample diagram for two-photon exchange contribution involving a qqq correlator. Such diagrams contribute to the leading power of the SSA for a transversely polarized target.

the aforementioned relation between the $q\gamma q$ correlator and the ETQS matrix element T_F , numerical results for A_{UT}^p and A_{UT}^n , and some discussion on the implications of our results. We summarize our work in Sec. 4.

2 Photons coupling to the same quark

In order to give a reference point and to fix our notation, let us first recall the well-known unpolarized cross section for inclusive DIS in the parton model in the one-photon exchange approximation,

$$k'^0 \frac{d\sigma_{unp}}{d^3\vec{k}'} = \frac{4\alpha_{em}^2}{Q^4 y} \left(1 - y + \frac{y^2}{2}\right) \sum_q e_q^2 x f_1^q(x) = \frac{2\alpha_{em}^2 y}{Q^4} \frac{\hat{s}^2 + \hat{t}^2}{\hat{u}^2} \sum_q e_q^2 x f_1^q(x), \quad (3)$$

where f_1^q denotes the unpolarized twist-2 quark distribution for a quark flavor q . A summation over both quarks and antiquarks is understood in Eq. (3). We make use of the common DIS variables

$$Q^2 = -(k - k')^2, \quad x = \frac{Q^2}{2P \cdot (k - k')}, \quad y = \frac{P \cdot (k - k')}{P \cdot k}. \quad (4)$$

Upon neglecting the nucleon mass, the variables in (4) are related through $y = Q^2/(xs)$, with $s = 2P \cdot k$ denoting the squared center-of-mass energy of the reaction. The (longitudinal) momentum of the struck quark is given by $p = xP$ (see also Fig. 1). In Eq. (3) we also use the partonic Mandelstam variables for the elastic lepton-quark scattering,

$$\hat{s} = (xP + k)^2 = \frac{Q^2}{y}, \quad \hat{t} = (xP - k')^2 = -\frac{Q^2(1-y)}{y}, \quad \hat{u} = (k - k')^2 = -Q^2, \quad (5)$$

which satisfy $\hat{s} + \hat{t} + \hat{u} = 0$.

We now turn to the transverse SSA for a polarized lepton beam. A nonzero spin asymmetry arises when taking into account the two-photon exchange contribution shown on the left panel of Fig. 1. The essential element of the calculation is the imaginary part of the lepton-quark box diagram which, in principle, was already computed in 1960 [18]. The real part of that diagram does not contribute to the SSA. The result for the spin-dependent cross section reads [10]

$$k'^0 \frac{d\sigma_{pol}^\ell}{d^3\vec{k}'} = \frac{4\alpha_{em}^3}{Q^8} m_\ell x y^2 \varepsilon^{S_\ell P k k'} \sum_q e_q^3 x f_1^q(x), \quad (6)$$

where we use the shorthand notation of Eq. (1) and the convention $\varepsilon^{0123} = 1$. The expression in (6) is proportional to the lepton mass m_ℓ , and, therefore, the general behavior of the spin asymmetry is given by $A_{UT}^\ell \sim \alpha_{em} m_\ell / Q$. This implies that even for DIS with a muon beam A_{UT}^ℓ should at best be of $\mathcal{O}(10^{-3})$. Although the asymmetry is suppressed like $1/Q$, the leading twist unpolarized quark distributions for the nucleon enter, while the suppression is caused by the lepton side of the process.

Computing A_{UT} for a nucleon target on the basis of the diagram on the left panel of Fig. 1 is more involved since this observable is a genuine twist-3 effect. One has contributions related to (i) collinear twist-3 correlators in the nucleon, (ii) transverse quark motion, and (iii) the quark mass. The calculation provides the cross section [10]²

$$k'^0 \frac{d\sigma_{pol}^N}{d^3\vec{k}'} = \frac{4\alpha_{em}^3}{Q^8} \frac{Mx^2y}{1-y} \varepsilon^{SNPkk'} \sum_q e_q^3 \left[\left(xg_T^q(x) - g_{1T}^{(1)q}(x) - \frac{m_q}{M} h_1^q(x) \right) \times \left((1-y)^2 \ln \frac{Q^2}{\lambda^2} + y(2-y) \ln y + y(1-y) \right) + \frac{m_q}{M} h_1^q(x) y(1-y) \right] + \dots, \quad (7)$$

which is proportional to the nucleon mass M . This result contains the collinear twist-3 two-parton correlator g_T which can also be measured, for instance, through the longitudinal-transverse double spin asymmetry A_{LT} in inclusive DIS. The contribution due to transverse quark motion is described by the correlator $g_{1T}^{(1)}$. This correlation function represents a particular moment of the transverse momentum dependent parton distribution g_{1T} [19, 20],

$$g_{1T}^{(1)}(x) = \int d^2\vec{p}_T \frac{\vec{p}_T^2}{2M^2} g_{1T}(x, \vec{p}_T^2). \quad (8)$$

In Eq. (7) the term proportional to the quark mass is described by the transversity distribution h_1 [21]. We point out that the transversity contribution to $d\sigma_{pol}^N$ was first published in Ref. [11]. In that work a projection operator for transversity was used which contains m_q . Then the calculation becomes identical to the case of a polarized lepton beam discussed above, and the full transversity-related result is just given by the very last term in Eq. (7). In contrast, the transversity contribution in (7) is obtained using a projection operator without a quark mass term. As we argue below, the *complete* result for the spin-dependent cross section does not depend on the choice of this projector.

The calculation leading to (7) satisfies electromagnetic gauge invariance, yet the result contains an uncancelled IR divergence. This divergence can be regularized by a photon mass λ which shows up in the logarithm $\ln(Q^2/\lambda^2)$ [10]. (Terms vanishing in the limit $\lambda \rightarrow 0$ are not listed in (7).) This feature clearly hints at additional contributions that also have to be taken into account. Indeed, since we are dealing with a twist-3 observable, one has to consider qqq correlations in the nucleon. The dots in (7) indicate these missing contributions, and a sample diagram is shown on the right panel of Fig. 1. (Diagrams where one of the exchanged photons is *real* can also contribute to the target SSA. However, they do not matter for the mentioned IR divergence.) It has been speculated that the inclusion of such terms could ultimately generate an IR-finite result [10, 11]. The twist-3 correlator which is relevant for the discussion of the IR divergence is denoted by \tilde{g}_T in Refs. [19, 20]. Through QCD equations of motion this function is related to the parton correlators showing up in (7) [19, 20],

$$x\tilde{g}_T(x) = xg_T(x) - g_{1T}^{(1)}(x) - \frac{m_q}{M} h_1(x). \quad (9)$$

Since the IR-divergent term in Eq. (7) appears with exactly the linear combination of parton correlators showing up on the r.h.s. of Eq. (9), it is justified to expect that the inclusion of the \tilde{g}_T term will

²The contribution depending on the quark mass m_q in Eq. (7) was not yet given in [10].

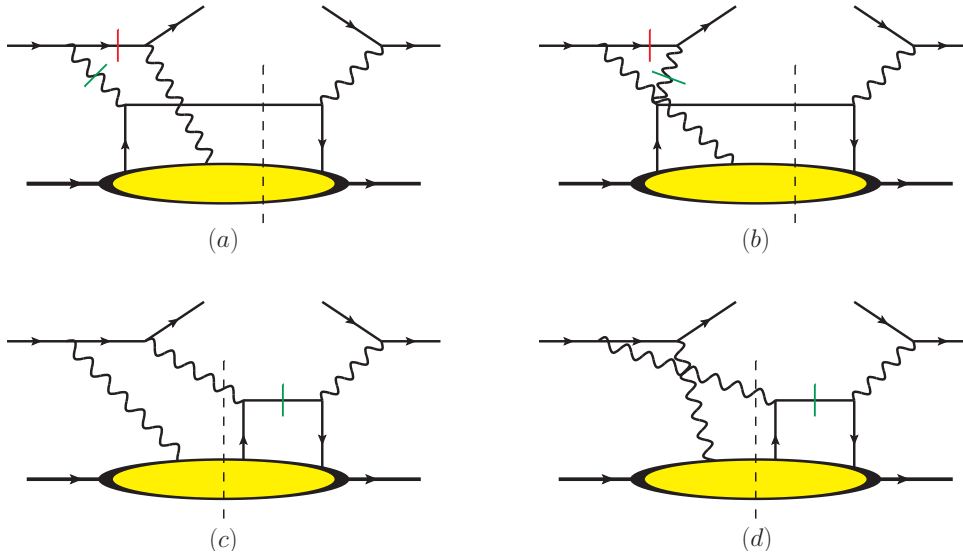


Figure 2: Two-photon exchange contributions to inclusive DIS where the photons couple to different quarks. (The Hermitian conjugate diagrams are not shown.) Such contributions can be expressed through a $q\gamma q$ correlator in the nucleon. Particle lines that can go on-shell are indicated by a short dash (see text for more details).

provide an IR-finite result. In fact, we were able to show that the IR divergence indeed cancels after taking into account all contributions (with virtual photon exchange), and currently we are working towards a complete result [22]. Let us also mention that the transversity-related quark mass term can be expected to be small because of the relative prefactor m_q/M . Actually, it was found that both A_{UT}^p and A_{UT}^n , based on the transversity contribution only, are just of $\mathcal{O}(10^{-4})$ even when using a constituent quark mass [11]. We note in passing that the quark mass term in (9) is absent if one works with the projection operator for transversity used in [11]. This shows that indeed both transversity projectors lead to the same final result for the spin-dependent cross section.

3 Photons coupling to different quarks

3.1 Analytical results

Now we consider the case where the two photons couple to different quarks in the nucleon — see Fig. 2 for the relevant Feynman diagrams. For the target SSA such diagrams contribute to the same order in $1/Q$ as those discussed in the previous section. Note, however, that they are not relevant for the dominant term of the lepton SSA. Therefore, the result in Eq. (6) represents the complete leading power expression for $d\sigma_{pol}^\ell$.

Imaginary parts are a necessary condition for the existence of SSAs. In Feynman graphs they generally arise when internal particles go on-shell, i.e., when one hits the pole of a particle propagator. For the diagrams in Fig. 2 there are two sources of such poles: first, the lepton propagators in diagrams (a) and (b) go on-shell if the longitudinal momentum of the photon coupling to the spectator quarks vanishes (soft photon pole). Second, particle propagators can go on-shell for a vanishing quark momentum (soft fermion pole). This applies to one photon propagator in diagrams (a) and (b), and to the quark propagator in diagrams (c) and (d). It turns out, however, that the soft fermion pole

contribution vanishes when summing over all diagrams. Specifically, the contributions from diagrams (a) and (d) cancel each other out, and similarly for diagrams (b) and (c). In this context we also refer to [23] where such a cancellation has already been discussed.

The bottom part of the diagrams in Fig. 2 is expressed through a $q\gamma q$ correlator. The discussion in the previous paragraph implies that we need this correlator only for the specific case of zero photon momentum. Following the conventions of Ref. [24] we define the relevant soft photon pole matrix element F_{FT} according to

$$\int \frac{d\xi^- d\zeta^-}{2(2\pi)^2} e^{ixP^+\xi^-} \langle P, S | \bar{\psi}^q(0) \gamma^+ e^{F_{QED}^+}(\zeta) \psi^q(\xi) | P, S \rangle = -M \varepsilon_T^{ij} S_T^j F_{FT}^q(x, x), \quad (10)$$

with $\varepsilon_T^{ij} \equiv \varepsilon^{-+ij}$ ($\varepsilon_T^{12} = 1$), and $e > 0$ denoting the elementary charge. The photon is represented by a component of the electromagnetic field strength tensor. The two arguments in F_{FT} indicate the longitudinal quark momenta, which become equal for a vanishing photon momentum. Note that in Eq. (10) Wilson lines between the field operators have been suppressed.

The $q\gamma q$ correlator F_{FT} is the QED counterpart of the ETQS soft gluon pole matrix element T_F [13–15]. In the notation of [15, 17, 25], T_F is specified through

$$\int \frac{d\xi^- d\zeta^-}{4\pi} e^{ixP^+\xi^-} \langle P, S | \bar{\psi}^q(0) \gamma^+ F_{QCD}^+(\zeta) \psi^q(\xi) | P, S \rangle = -\varepsilon_T^{ij} S_T^j T_F^q(x, x). \quad (11)$$

For later convenience we also recall the model-independent relation between T_F and the transverse momentum dependent Sivers function $f_{1T}^\perp(x, \vec{p}_T^2)$ [26]. Taking the Sivers function as defined in semi-inclusive DIS (see, e.g., Ref. [20]) one has [25, 27, 28]

$$-g T_F(x, x) = \int d^2\vec{p}_T \frac{\vec{p}_T^2}{M} f_{1T}^\perp(x, \vec{p}_T^2) \Big|_{SIDIS}, \quad (12)$$

with g denoting the strong coupling constant. If one instead considers the Sivers function appropriate for the Drell-Yan process the sign on the l.h.s. in Eq. (12) has to be reversed [29, 30]. Furthermore, note that by definition the Sivers function and $g T_F$ do not depend on the sign of the strong coupling constant whereas T_F does.

Let us now return to the target SSA A_{UT}^N . The soft photon pole contribution from diagrams (a) and (b) in Fig. 2 gives rise to the following polarized cross section³:

$$k'^0 \frac{d\sigma_{pol}^N}{d^3\vec{k}'} = \frac{8\pi\alpha_{em}^2 xy^2 M}{Q^8} \frac{\hat{s}^2 + \hat{t}^2}{\hat{u}^2} \left(2 + \frac{\hat{u}}{\hat{t}}\right) \varepsilon^{S_N P k k'} \sum_q e_q^2 x \tilde{F}_{FT}^{q/N}(x, x), \quad (13)$$

$$\text{with } \tilde{F}_{FT}(x, x) = F_{FT}(x, x) - x \frac{d}{dx} F_{FT}(x, x).$$

We performed the calculation both in the Feynman gauge and in the light-cone gauge in the collinear twist-3 approach. We also compared the result to Ref. [17] where, in particular, the soft gluon pole contribution to the transverse SSA for the process $p^\uparrow p \rightarrow \pi X$ was studied. Specifically, if one takes from that paper the result for the $qq' \rightarrow q'q$ channel, strips off the respective color factors, and pays attention to the sign conventions, one finds complete agreement between both calculations. Note that for the QED treatment of the present work the overall sign of the polarized cross section is uniquely determined, since the sign of the photon-lepton coupling is fixed by means of the covariant derivative $D^\mu = \partial^\mu - ieA^\mu$. The so-called derivative term of the result, given by $(d/dx)F_{FT}$, and the non-derivative term, given by F_{FT} , have the same hard scattering coefficient, which is typical

³We use here the same symbol for the polarized cross section as in Eq. (7) in order to avoid a proliferation of symbols.

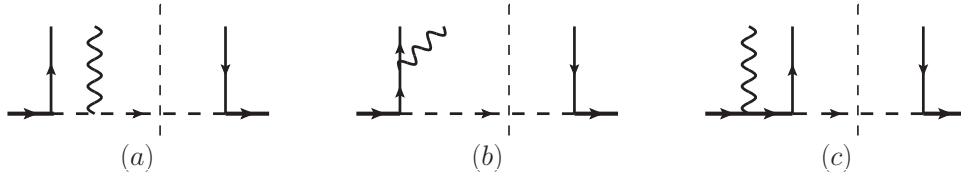


Figure 3: Feynman diagrams for the $q\gamma q$ -correlation function F_{FT} in a diquark model of the nucleon. Diagram (c) has to be considered in the case of the proton. Only diagram (a) gives a nonzero contribution.

for such types of calculations [17,31]. If the momentum fraction x is sufficiently large the derivative term numerically dominates over the non-derivative term [14,15]. Like the unpolarized cross section in Eq. (3), the expression in (13) contains an explicit factor of α_{em}^2 . In addition, when evaluated, F_{FT} is proportional to α_{em} so that the polarized cross section is actually proportional to α_{em}^3 and hence suppressed.

On the basis of the polarized cross section in Eq. (13) and the unpolarized cross section in Eq. (3), one can evaluate the SSA in Eq. (2). We compute A_{UT}^N in the target rest frame where one finds $\varepsilon^{SNPkk'} = M\vec{S} \cdot (\vec{k} \times \vec{k}')$. The lepton beam points along the negative z direction ($\hat{k} = -\hat{e}_z$), the (xz) plane represents the lepton plane (where \vec{k}' has a positive x component), and the y direction is defined according to $\hat{e}_y = \hat{e}_z \times \hat{e}_x$. In that case the SSA is given by

$$A_{UT}^N = \frac{d\sigma(\uparrow_y) - d\sigma(\downarrow_y)}{2d\sigma_{unp}} = -\frac{2\pi M}{Q} \frac{2-y}{\sqrt{1-y}} \frac{\sum_q e_q^2 x \tilde{F}_{FT}^{q/N}(x, x)}{\sum_q e_q^2 x f_1^{q/N}(x)}, \quad (14)$$

with \uparrow_y (\downarrow_y) denoting polarization of the nucleon along \hat{e}_y ($-\hat{e}_y$). In Sec. 3.3 we will show numerical results for A_{UT}^N .

3.2 Relation between $q\gamma q$ correlator and qgq correlator

We need some input for the $q\gamma q$ correlator F_{FT} in order to obtain an estimate for A_{UT}^N . To proceed we restrict ourselves to the large- x valence quark region, i.e., we neglect in particular contributions from antiquarks. For the comparison with the data from HERMES [6] and JLab [8] this approximation should be justified. Let us first assume that the two spectator quarks can be described through a single diquark. In such a diquark model of the nucleon, F_{FT} is given by the diagrams in Fig. 3. It turns out that only diagram (a) gives a nonzero contribution. By explicit calculation one can show that diagram (b) vanishes. For a scalar diquark this was already pointed out in Ref. [32], while we extended this study to a vector diquark. Moreover, also diagram (c) does not contribute to the soft photon pole matrix element as can readily be shown using contour integration. These results hold for both a pointlike nucleon-quark-diquark vertex and a vertex containing an (arbitrary) form factor.

Since we are left with diagram (a) only, one can establish a simple relation between F_{FT} and the ETQS matrix element T_F for which the same graph has to be computed with the photon replaced by a gluon. The precise form of the relation for a given quark and nucleon mainly depends on the strong coupling and the electromagnetic charge of the diquark. One obtains

$$\begin{aligned} F_{FT}^{u/p} &= -\frac{\alpha_{em}}{6\pi C_F \alpha_s M} (g T_F^{u/p}), & F_{FT}^{d/p} &= -\frac{2\alpha_{em}}{3\pi C_F \alpha_s M} (g T_F^{d/p}), \\ F_{FT}^{u/n} &= \frac{\alpha_{em}}{3\pi C_F \alpha_s M} (g T_F^{d/p}), & F_{FT}^{d/n} &= -\frac{\alpha_{em}}{6\pi C_F \alpha_s M} (g T_F^{u/p}), \end{aligned} \quad (15)$$

where $C_F = 4/3$. Note that for $T_F^{q/N}$ we used isospin symmetry. We assumed a pointlike coupling between the gauge bosons and the diquark. Since the gauge boson has a vanishing (longitudinal) momentum this assumption appears reasonable to us. We point out that exactly the same relations between F_{FT} and T_F are valid in a more general 3-quark picture of the nucleon. To arrive at this result one merely needs the fact that it does not matter to which of the two spectator quarks the gauge boson couples. This obviously holds if the spectator quarks have the same flavor, but it also applies in the case of different flavors [33]⁴. If higher order corrections are taken into consideration the simple relations in (15) break down. However, we do not expect such corrections to affect the general conclusions drawn in Sec. 3.3. We also mention that, when computing the target SSAs, we evaluate the strong coupling constant appearing in (15) at the scale $\mu^2 = Q^2$.

Before discussing the numerical results we briefly explain why the diagrams with the photons coupling to different quarks presumably dominate over those considered in Sec. 2. The total contribution to the polarized cross section, caused by the diagrams where the photons couple to the same quark, is proportional to α_{em}^3 multiplied by ggq correlators like gT_F [22]. (Here we neglect the transversity-related quark mass term.) This, however, is suppressed by a factor α_s compared to the diagrams in Fig. 2 — see Eqs. (13) and (15). Though one might argue that this factor α_s should be evaluated in the non-perturbative regime it may well give rise to a numerical suppression. Second, it has been shown that for elastic lepton-nucleon scattering photons coupling to different quarks even dominate in a $1/Q$ expansion over those coupling to the same quark [34, 35]. (This finding is equivalent to the so-called Landshoff mechanism for elastic scattering of hadrons at large momentum transfer [36].) Therefore, one may expect a similar behavior for inclusive DIS in the region of larger values of x . Of course, only a full calculation of the diagrams containing ggq correlations [22] will provide an ultimate answer on this point.

3.3 Numerical results and discussion

For our numerical estimates we have used three inputs for the $q\gamma q$ correlator F_{FT} based on three different extractions of T_F :

- **Sivers** input: This input uses an indirect extraction of T_F based on the Sivers functions obtained from HERMES [37] and COMPASS [38] data on production of pions and kaons in semi-inclusive DIS [39], and the relation in Eq. (12) between f_{1T}^\perp and T_F .
- **KQVY** input: This input uses a direct extraction of T_F by Kouvaris, Qiu, Vogelsang, and Yuan (KQVY) [17], based on Fermilab data ($\sqrt{s} \approx 20$ GeV) for $p^\uparrow p \rightarrow \pi X$ and $\bar{p}^\uparrow p \rightarrow \pi X$ [40], and RHIC data ($\sqrt{s} = 200$ GeV) from STAR [41, 42] (for $p^\uparrow p \rightarrow \pi X$) and BRAHMS [43] (for $p^\uparrow p \rightarrow \pi X$ and $p^\uparrow p \rightarrow \eta X$). (See also Ref. [44] for the most recent STAR data on $p^\uparrow p \rightarrow \pi X$ and $p^\uparrow p \rightarrow \eta X$.) We took into account the sign error of that extraction [25]. Also, we used Fit I in Ref. [17] which contains valence quarks only. Our general conclusions would not change if we used Fit II from [17] where sea quarks are considered as well. It has been pointed out that the Sivers and the KQVY extractions of T_F disagree in sign [25]. Currently, this sign mismatch issue represents a key puzzle in hadronic spin physics. Below we will come back to that puzzle.
- **KP** input: This input also uses an indirect extraction of T_F based on a new fit of the Sivers function by Kang and Prokudin (KP) [45], and the relation in Eq. (12). The authors of [45] attempted a simultaneous fit of recent HERMES [46] and COMPASS [47] data on pion production in semi-inclusive DIS, as well as RHIC data on $p^\uparrow p \rightarrow \pi X$ [42, 43]. They allowed for the Sivers function to have a node in x and in p_T — see also the recent work [48, 49] where a node of f_{1T}^\perp

⁴We also acknowledge a discussion with C. Lorcé and B. Pasquini about that point.

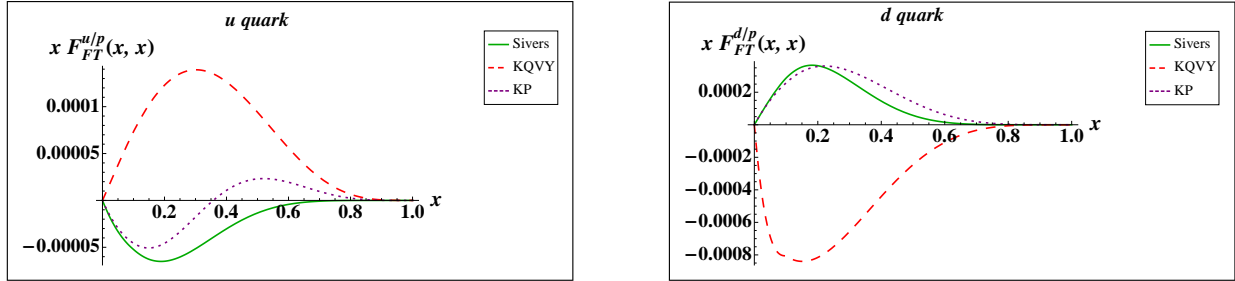


Figure 4: Numerical result for our model for the $q\gamma q$ correlator F_{FT} for the proton at the scale $\mu^2 = 2 \text{ GeV}^2$, based on three different inputs for T_F . Left panel: Up quarks. Right panel: Down quarks.

in x was discussed. Even when considering such nodes it was found that, with the Siverts effect alone, no satisfactory combined description of SSAs in semi-inclusive DIS and in proton-proton collisions can be achieved. In other words, Siverts functions with nodes do not help to resolve the aforementioned sign mismatch problem.

The numerical results for F_{FT} for the proton are shown in Fig. 4. The neutron results can be obtained immediately from these plots too since, according to (15), one has $F_{FT}^{u/n} = -F_{FT}^{d/p}/2$ and $F_{FT}^{d/n} = F_{FT}^{u/p}$. In general, the magnitude of F_{FT} is rather small, which is mainly due to the factor α_{em} showing up in (15). The opposite sign for the Siverts input and the KQVY input nicely reflects the sign mismatch holding for both up quarks and down quarks [25]. Also, notice the node in $F_{FT}^{u/p}$ for the KP input which is a direct consequence of a node in the up quark Siverts function [45] — see Eqs. (15) and (12). Because of this node, the KP fits for $f_{1T}^{\perp u/p}$ and $f_{1T}^{\perp d/p}$ have the same sign at larger values of x [45]. Such a scenario is actually at variance with a model-independent large- N_c analysis [50].

Let us now turn our attention to the target asymmetry in Eq. (14). When computing the asymmetries, for the unpolarized parton densities f_1^q we take the GRV98 parametrization [51] for the Siverts input and the KP input, whereas we take the CTEQ5L parametrization [52] in the case of the KQVY input. Those parametrizations were the ones used in the respective fits. The results for A_{UT}^p are displayed in Fig. 5. From the plot on the left panel of that figure we see that the Siverts input perfectly agrees with the HERMES data. Overall, also the KQVY and the KP inputs give a good description of the data. One may, however, sense from the plot that these two inputs become somewhat too large towards larger x . In the KP case this is due to the aforementioned node in $f_{1T}^{\perp u/p}$. Therefore, our results indicate that such a node is not preferred, even though it is not ruled out by the current data either. The plot on the right panel of Fig. 5 shows results for typical HERMES kinematics extending until $x = 0.8$. This figure suggests that sufficiently precise data for A_{UT}^p at such large x values may allow one to distinguish between the different inputs for F_{FT} and, hence, the different inputs for T_F . (Of course, here one has to keep in mind that also the Siverts input is hardly constrained for $x > 0.4$ [37–39].) We note that the KP input actually provides a finite asymmetry in the limit $x \rightarrow 1$, while for the KQVY input the asymmetry diverges in that limit. In this context we would like to add the following point: in general, if one fits available data on SSAs in processes like $p^\uparrow p \rightarrow \pi X$ by means of the Siverts effect (as described in the twist-3 collinear framework) alone, then the resulting T_F typically is such that the asymmetry violates the positivity bound for $x_F \rightarrow 1$ [17, 53]. (Note that if the so extracted T_F is used to compute SSAs for other processes, the positivity bound may be violated already at lower values of x_F — in this context, see for instance [54].) This phenomenon, which is caused by the strong rise of the measured asymmetries towards larger values of x_F , gives some hint

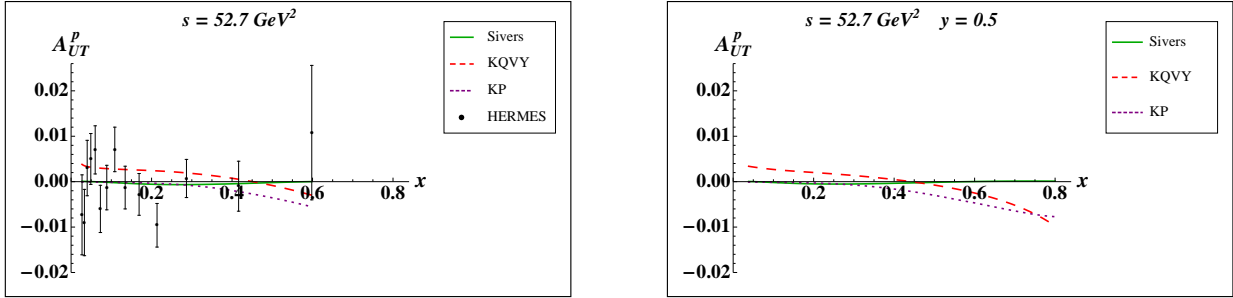


Figure 5: Proton target asymmetry for three inputs for F_{FT} . Left panel: Comparison to data from the HERMES Collaboration [6]. The asymmetry has been evaluated for the average values $\langle x \rangle$ and $\langle Q^2 \rangle$ of the data bins. Right panel: Results for typical HERMES kinematics at $y = 0.5$, where the lowest x value for the curves corresponds to $Q^2 = 1 \text{ GeV}^2$.

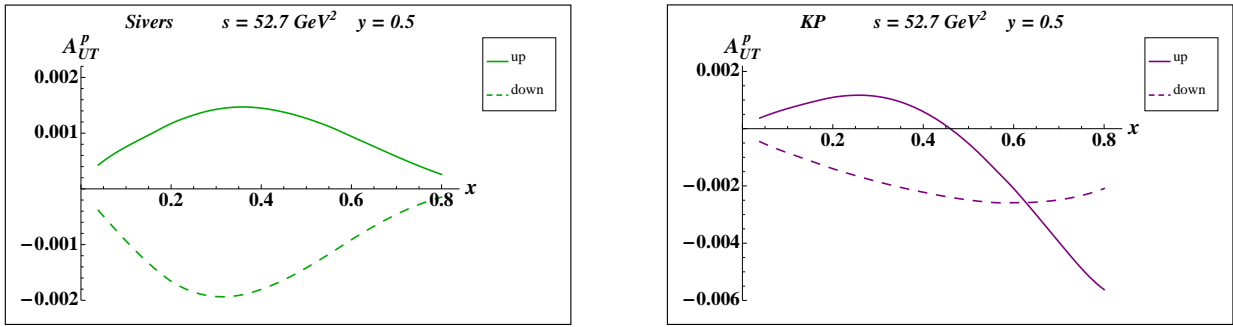


Figure 6: Individual flavor contributions to the proton asymmetry for the Siverts input (left panel) and the KP input (right panel). The results are for typical HERMES kinematics at $y = 0.5$, where the lowest x value for the curves corresponds to $Q^2 = 1 \text{ GeV}^2$.

that the twist-3 Siverts-type effect may not be the only cause of the observed SSAs. As we discuss in more detail below, the data on the neutron SSA in inclusive DIS clearly support this point of view.

Before moving on to the neutron case it is instructive to look at the individual flavor contributions to A_{UT}^p which are shown for the Siverts and KP inputs in Fig. 6. In the Siverts case these individual contributions are quite small and, moreover, they almost exactly cancel each other. This explains the tiny effect we find for A_{UT}^p . (Note that other available extractions of the Siverts functions from data on semi-inclusive DIS [49, 55–60] lead to a similarly small effect for A_{UT}^p .) For the KP input there is also a partial cancellation among the flavor contributions at lower values of x , whereas at larger x , because of the node in x in $f_{1T}^{\perp u/p}$, up quark and down quark contributions give rise to the same sign.

In Fig. 7, the results for the neutron asymmetry A_{UT}^n are shown. While the plot on the left panel of that figure is for the kinematics of the E07-013 experiment in Hall A at Jefferson Lab [7, 8], the one on the right panel shows results for typical Jefferson Lab kinematics at fixed values of y covering a larger x range. We refrain from including in the plot the data given in Ref. [8], since final data from the Hall A Collaboration should be available soon [61]. The (preliminary) data from [8] on A_{UT}^n are on the (few) percent level and positive. In fact the Siverts and KP inputs agree reasonably well with these data. (In the x region of the current data both inputs actually provide almost identical results and differences become manifest only towards larger x — see plot on the right panel of Fig. 7.) This means, in particular, that we have a framework which can simultaneously describe both the vanishing/tiny

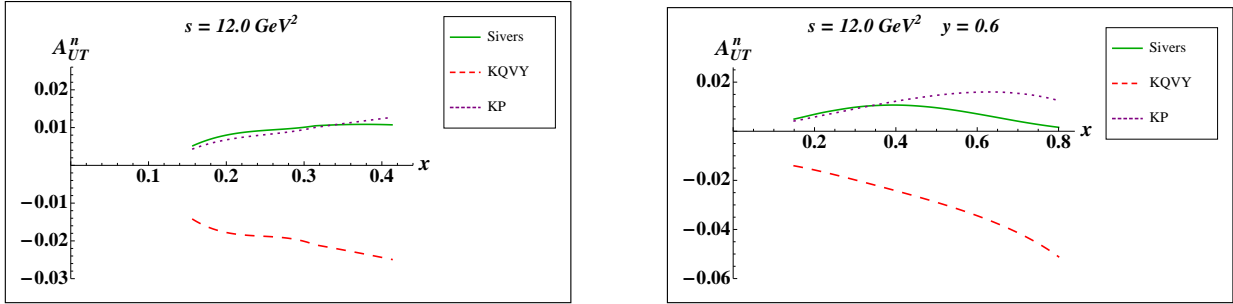


Figure 7: Neutron target asymmetry for three inputs for F_{FT} . Left panel: Calculation for kinematics of the experiment in Hall A at Jefferson Lab [7,8]. The asymmetry has been evaluated for the average values $\langle x \rangle$ and $\langle Q^2 \rangle$ of the data bins. The preliminary result for A_{UT}^n is positive and on the (few) percent level [8]. Right panel: Results for typical Jefferson Lab kinematics at $y = 0.6$, where the lowest x value for the curves corresponds to $Q^2 = 1 \text{ GeV}^2$.

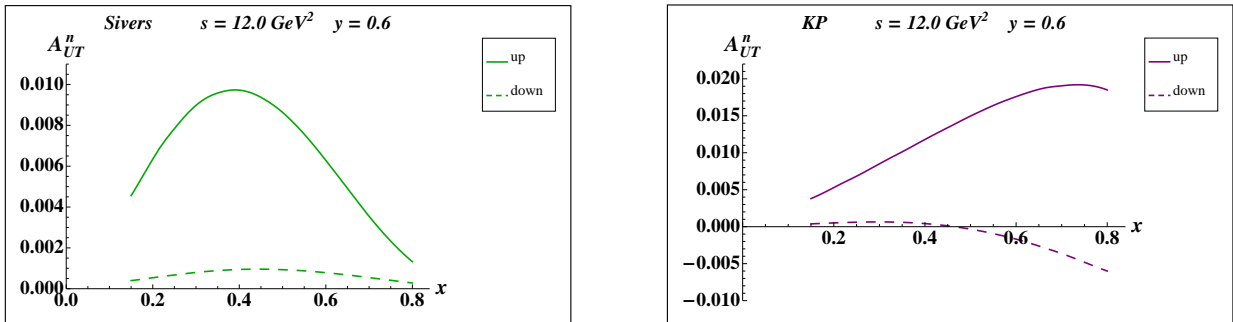


Figure 8: Individual flavor contributions to the neutron asymmetry for the Siverts input (left panel) and the KP input (right panel). The results are for typical Jefferson Lab kinematics at $y = 0.6$, where the lowest x value for the curves corresponds to $Q^2 = 1 \text{ GeV}^2$.

result for A_{UT}^p as well as the nonzero result for A_{UT}^n . The plots of the individual flavor contributions in Fig. 8 show that the neutron asymmetry is dominated by the (relatively large) up quark contribution.

Notice that if we had a node in p_T in the Siverts function such that f_{1T}^\perp (at low p_T) and the particular p_T moment of the Siverts function on the r.h.s. in Eq. (12) have opposite signs, we would obtain the wrong sign for the neutron asymmetry from the Siverts input. Such a node was suggested in Ref. [25] as a potential resolution of the sign mismatch problem. However, as a result of a more detailed phenomenological work, it was already pointed out in Ref. [45] that a node of the Siverts function in p_T can hardly solve the sign mismatch issue. Our finding here is in line with that observation.

An additional crucial lesson from the neutron data is that the KQVY input gives us the wrong sign for A_{UT}^n . This suggests that the SSAs seen in processes like $p^\uparrow p \rightarrow \pi X$ are not mainly caused by the Siverts mechanism as described in twist-3 collinear factorization. Therefore, the sign mismatch problem boils down to the question about the origin of the SSAs in those reactions. One popular alternative mechanism considered in the literature is the Collins effect [62] (or its collinear twist-3 analog), which describes a transverse SSA in parton fragmentation. For instance, in a recent study carried out in a generalized (transverse momentum dependent) parton model it was argued that the Collins effect can contribute significantly but is not sufficient to entirely describe the observed effects [63]. This is an important result even though the existing papers on this topic — see [63–65] and references therein

— do not allow one to draw an ultimate conclusion about the role of the fragmentation-related contribution to SSAs in hadronic collisions. Other mechanisms have been proposed as well [66–69], and more work is required in order to settle this important question.

Let us also remark that at least a qualitative simultaneous description of SSAs in semi-inclusive DIS and in hadronic collisions can be achieved if one merely assumes the existence of a Siverson function without relating f_{1T}^\perp to the rescattering of active partons with beam remnants [70, 71]. In such a scenario, in particular, one does not face a sign mismatch problem between the different processes. However, if the rescattering picture, which also underlies the current definition of transverse momentum dependent parton distributions in QCD [29, 72], is taken seriously, then the sign mismatch problem cannot be circumvented [17, 25, 73, 74]. The fact that in the present work we can describe SSAs in inclusive DIS using the Siverson function extracted from semi-inclusive DIS does support the rescattering picture underlying the Siverson effect — see diagrams (a) and (b) in Fig. 2. Obviously, our analysis also supports that the observed so-called $\sin(\phi_h - \phi_S)$ modulation of the cross section for semi-inclusive DIS can indeed be associated with the Siverson function.

Finally, we briefly comment on two potential error sources of our numerical results in addition to those caused, e.g., by the model for the $q\gamma q$ correlator F_{FT} . First, the three different extractions of T_F that we are using have uncertainties. However, only for the Siverson input is a quantitative error estimate available [39]. Since the neutron asymmetry is almost entirely determined by the down quark Siverson function for the proton — see plot on the left panel of Fig. 8 as well as Eq. (15) — the error for A_{UT}^n in the case of the Siverson input corresponds to the error for $f_{1T}^{\perp d/p}$. According to Ref. [39] the error for $f_{1T}^{\perp d/p}$, in the x range of the Jefferson Lab data, is roughly of the order $\pm(30 - 50)\%$ with the larger uncertainty towards larger values of x . This suggests that the Siverson input leads to a robust prediction of a positive A_{UT}^n . Second, target mass corrections may play a role, especially for the Jefferson Lab kinematics. While it is definitely worth trying to obtain an estimate of such corrections, a corresponding study would go beyond the scope of this work, not the least because at present there exists no generally accepted framework for treating target mass corrections in DIS — see Refs. [75–79] for detailed recent work on this topic. Moreover, since the polarized cross section entering A_{UT} is a twist-3 observable, it is not clear if any of the proposed frameworks in the literature would be directly applicable. Target mass corrections might also cancel to a large extent in the spin asymmetry.

4 Summary

In summary, we have investigated transverse SSAs in inclusive DIS off the nucleon with a focus on the target SSA, which recently has been measured for a proton target [6] and a neutron target [7, 8]. Such observables can exist only if more than one photon is exchanged between the leptonic and the hadronic part of the process. In the present work we have considered two-photon exchange where the two photons couple to *different* quarks inside the nucleon, and we have given arguments why this mechanism presumably dominates over two photons coupling to the *same* quark considered in Refs. [10, 11, 22].

Our calculation has been carried out in the collinear twist-3 approach and contains a quark-photon-quark correlator (denoted by F_{FT}) of the nucleon. We have shown that in a valence quark picture of the nucleon F_{FT} is related to the Efremov-Teryaev-Qiu-Sterman quark-gluon-quark correlator T_F . The function T_F has a model-independent relation to the transverse momentum dependent Siverson function f_{1T}^\perp and plays a crucial role in the QCD description of SSAs for processes like $p^\uparrow p \rightarrow \pi X$.

The relation between F_{FT} and T_F has allowed us to numerically compute the target SSA in inclusive DIS. We have found a reasonable description of both the proton data and the (preliminary)

neutron data, provided that we take T_F obtained from a fit of the Sivers function to data in semi-inclusive DIS [39]. Our analysis also indicates that a node of f_{1T}^\perp in x is not preferred, though it is not ruled out either by the currently available data. We also argued that a node of the Sivers function in the transverse momentum p_T such that f_{1T}^\perp (at low p_T) and the p_T moment of f_{1T}^\perp on the r.h.s. in Eq. (12) have opposite signs, would not work — see also Ref. [45]. Moreover, our study suggests that the nonzero $\sin(\phi_h - \phi_S)$ modulation observed in semi-inclusive DIS can be attributed to the Sivers function and, in particular, supports the understanding that the Sivers effect is intimately related to the reinteraction of active partons with target remnants. If we take T_F based on a direct extraction from SSAs in hadronic collisions [17, 25], we obtain the wrong sign for the neutron asymmetry in inclusive DIS. This finding indicates that the Sivers effect cannot be the only source of the SSAs observed in processes like $p^\uparrow p \rightarrow \pi X$. Keeping in mind the large spin effects (up to 50%) measured there, it is of crucial importance to eventually settle what causes these asymmetries.

Acknowledgments: We are grateful to J. Katich for sending us his Ph.D. thesis. Moreover, we thank D. Hasch, A. López Ruiz, A. Martínez de la Ossa, and G. Schnell for a discussion about the sign conventions of the HERMES data, and J.-P. Chen for a discussion about the data from Jefferson Lab. This work has been supported in part by the NSF under Grant No. PHY-0855501, and by the BMBF under Grant No. OR 06RY9191.

References

- [1] N. Christ and T. D. Lee, Phys. Rev. **143**, 1310 (1966).
- [2] M. K. Jones *et al.* [Jefferson Lab Hall A Collaboration], Phys. Rev. Lett. **84**, 1398 (2000) [nucl-ex/9910005].
- [3] J. Arrington, P. G. Blunden and W. Melnitchouk, Prog. Part. Nucl. Phys. **66**, 782 (2011) [arXiv:1105.0951 [nucl-th]].
- [4] J. R. Chen *et al.*, Phys. Rev. Lett. **21**, 1279 (1968); J. A. Appel *et al.*, Phys. Rev. D **1**, 1285 (1970).
- [5] S. Rock *et al.*, Phys. Rev. Lett. **24**, 748 (1970).
- [6] A. Airapetian *et al.* [HERMES Collaboration], Phys. Lett. B **682**, 351 (2010) [arXiv:0907.5369 [hep-ex]].
- [7] Jefferson Lab experiment E07-013; Spokespersons: T. D. Averett, T. Holmstrom, X. Jiang.
- [8] J. M. Katich, Ph.D. thesis, The College of William and Mary, 2011.
- [9] R. N. Cahn and Y.-S. Tsai, Phys. Rev. D **2**, 870 (1970).
- [10] A. Metz, M. Schlegel and K. Goeke, Phys. Lett. B **643**, 319 (2006) [hep-ph/0610112].
- [11] A. Afanasev, M. Strikman and C. Weiss, Phys. Rev. D **77**, 014028 (2008) [arXiv:0709.0901 [hep-ph]].
- [12] M. Schlegel and A. Metz, AIP Conf. Proc. **1149**, 543 (2009) [arXiv:0902.0781 [hep-ph]].
- [13] A. V. Efremov and O. V. Teryaev, Sov. J. Nucl. Phys. **36**, 140 (1982) [Yad. Fiz. **36**, 242 (1982)]; Phys. Lett. B **150**, 383 (1985).

- [14] J.-w. Qiu and G. F. Sterman, Phys. Rev. Lett. **67**, 2264 (1991); Nucl. Phys. B **378**, 52 (1992).
- [15] J.-w. Qiu and G. F. Sterman, Phys. Rev. D **59**, 014004 (1998) [hep-ph/9806356].
- [16] H. Eguchi, Y. Koike and K. Tanaka, Nucl. Phys. B **752**, 1 (2006) [arXiv:hep-ph/0604003]; Nucl. Phys. B **763**, 198 (2007) [arXiv:hep-ph/0610314].
- [17] C. Kouvaris, J. W. Qiu, W. Vogelsang and F. Yuan, Phys. Rev. D **74**, 114013 (2006) [arXiv:hep-ph/0609238].
- [18] A. O. Barut and C. Fronsdal, Phys. Rev. **120**, 1871 (1960).
- [19] P. J. Mulders and R. D. Tangerman, Nucl. Phys. B **461**, 197 (1996) [Erratum-ibid. B **484**, 538 (1997)] [hep-ph/9510301].
- [20] A. Bacchetta *et al.*, JHEP **0702**, 093 (2007) [hep-ph/0611265].
- [21] J. P. Ralston and D. E. Soper, Nucl. Phys. B **152**, 109 (1979).
- [22] M. Schlegel, work in progress.
- [23] Y. Koike, W. Vogelsang and F. Yuan, Phys. Lett. B **659**, 878 (2008) [arXiv:0711.0636 [hep-ph]].
- [24] S. Meissner, Ph.D. thesis, University of Bochum, 2009.
- [25] Z. -B. Kang, J. -W. Qiu, W. Vogelsang and F. Yuan, Phys. Rev. D **83**, 094001 (2011) [arXiv:1103.1591 [hep-ph]].
- [26] D. W. Sivers, Phys. Rev. D **41**, 83 (1990); Phys. Rev. D **43**, 261 (1991).
- [27] D. Boer, P. J. Mulders and F. Pijlman, Nucl. Phys. B **667**, 201 (2003) [hep-ph/0303034].
- [28] J. P. Ma and Q. Wang, Eur. Phys. J. C **37**, 293 (2004) [hep-ph/0310245].
- [29] J. C. Collins, Phys. Lett. B **536**, 43 (2002) [hep-ph/0204004].
- [30] S. J. Brodsky, D. S. Hwang and I. Schmidt, Nucl. Phys. B **642**, 344 (2002) [hep-ph/0206259].
- [31] Y. Koike and K. Tanaka, Phys. Rev. D **76**, 011502 (2007) [hep-ph/0703169].
- [32] Z. -B. Kang, J. -W. Qiu and H. Zhang, Phys. Rev. D **81**, 114030 (2010) [arXiv:1004.4183 [hep-ph]].
- [33] B. Pasquini and F. Yuan, Phys. Rev. D **81**, 114013 (2010) [arXiv:1001.5398 [hep-ph]].
- [34] D. Borisyuk and A. Kobushkin, Phys. Rev. D **79**, 034001 (2009) [arXiv:0811.0266 [hep-ph]].
- [35] N. Kivel and M. Vanderhaeghen, Phys. Rev. Lett. **103**, 092004 (2009) [arXiv:0905.0282 [hep-ph]].
- [36] P. V. Landshoff, Phys. Rev. D **10**, 1024 (1974).
- [37] M. Dieffenthaler [HERMES Collaboration], arXiv:0706.2242 [hep-ex].
- [38] A. Martin [COMPASS Collaboration], Czech. J. Phys. **56**, F33 (2006) [hep-ex/0702002].
- [39] M. Anselmino *et al.*, Eur. Phys. J. A **39**, 89 (2009) [arXiv:0805.2677 [hep-ph]].

- [40] D. L. Adams *et al.* [E581 and E704 Collaborations], Phys. Lett. B **261**, 201 (1991); D. L. Adams *et al.* [FNAL-E704 Collaboration], Phys. Lett. B **264**, 462 (1991); K. Krueger *et al.*, Phys. Lett. B **459**, 412 (1999).
- [41] J. Adams *et al.* [STAR Collaboration], Phys. Rev. Lett. **92**, 171801 (2004) [hep-ex/0310058].
- [42] B. I. Abelev *et al.* [STAR Collaboration], Phys. Rev. Lett. **101**, 222001 (2008) [arXiv:0801.2990 [hep-ex]].
- [43] I. Arsene *et al.* [BRAHMS Collaboration], Phys. Rev. Lett. **101**, 042001 (2008) [arXiv:0801.1078 [nucl-ex]].
- [44] L. Adamczyk *et al.* [STAR Collaboration], Phys. Rev. D **86**, 051101 (2012) [arXiv:1205.6826 [nucl-ex]].
- [45] Z. -B. Kang and A. Prokudin, Phys. Rev. D **85**, 074008 (2012) [arXiv:1201.5427 [hep-ph]].
- [46] A. Airapetian *et al.* [HERMES Collaboration], Phys. Rev. Lett. **103**, 152002 (2009) [arXiv:0906.3918 [hep-ex]].
- [47] M. Alekseev *et al.* [COMPASS Collaboration], Phys. Lett. B **673**, 127 (2009) [arXiv:0802.2160 [hep-ex]].
- [48] D. Boer, Phys. Lett. B **702**, 242 (2011) [arXiv:1105.2543 [hep-ph]].
- [49] A. Bacchetta and M. Radici, Phys. Rev. Lett. **107**, 212001 (2011) [arXiv:1107.5755 [hep-ph]].
- [50] P. V. Pobylitsa, hep-ph/0301236.
- [51] M. Gluck, E. Reya and A. Vogt, Eur. Phys. J. C **5**, 461 (1998) [hep-ph/9806404].
- [52] H. L. Lai *et al.* [CTEQ Collaboration], Eur. Phys. J. C **12**, 375 (2000) [hep-ph/9903282].
- [53] K. Kanazawa and Y. Koike, Phys. Rev. D **82**, 034009 (2010) [arXiv:1005.1468 [hep-ph]].
- [54] Y. Koike, AIP Conf. Proc. **675**, 449 (2003) [hep-ph/0210396].
- [55] A. V. Efremov *et al.*, Phys. Lett. B **612**, 233 (2005) [hep-ph/0412353].
- [56] M. Anselmino *et al.*, Phys. Rev. D **71**, 074006 (2005) [hep-ph/0501196]; Phys. Rev. D **72**, 094007 (2005) [Erratum-ibid. D **72**, 099903 (2005)] [hep-ph/0507181].
- [57] W. Vogelsang and F. Yuan, Phys. Rev. D **72**, 054028 (2005) [hep-ph/0507266].
- [58] J. C. Collins *et al.*, Phys. Rev. D **73**, 014021 (2006) [hep-ph/0509076].
- [59] S. Arnold *et al.*, arXiv:0805.2137 [hep-ph].
- [60] M. Anselmino, M. Boglione and S. Melis, Phys. Rev. D **86**, 014028 (2012) [arXiv:1204.1239 [hep-ph]].
- [61] T. D. Averett, J.-P. Chen, J. M. Katich, private communication, 2012.
- [62] J. C. Collins, Nucl. Phys. B **396**, 161 (1993) [hep-ph/9208213].
- [63] M. Anselmino *et al.*, Phys. Rev. D **86**, 074032 (2012) [arXiv:1207.6529 [hep-ph]].

- [64] Z. -B. Kang, F. Yuan and J. Zhou, Phys. Lett. B **691**, 243 (2010) [arXiv:1002.0399 [hep-ph]]; F. Yuan and J. Zhou, Phys. Rev. Lett. **103**, 052001 (2009) [arXiv:0903.4680 [hep-ph]].
- [65] Z. -B. Kang and F. Yuan, Phys. Rev. D **84**, 034019 (2011) [arXiv:1106.1375 [hep-ph]].
- [66] P. Hoyer and M. Jarvinen, JHEP **0702**, 039 (2007) [hep-ph/0611293].
- [67] P. Hoyer, M. Jarvinen and S. Kurki, JHEP **0810**, 086 (2008) [arXiv:0808.0626 [hep-ph]].
- [68] Y. Qian and I. Zahed, Phys. Rev. D **86**, 014033 (2012) [arXiv:1112.4552 [hep-ph]].
- [69] Y. V. Kovchegov and M. D. Sievert, Phys. Rev. D **86**, 034028 (2012) [arXiv:1201.5890 [hep-ph]].
- [70] M. Boglione, U. D'Alesio and F. Murgia, Phys. Rev. D **77**, 051502 (2008) [arXiv:0712.4240 [hep-ph]].
- [71] M. Anselmino *et al.*, arXiv:0907.3999 [hep-ph].
- [72] S. J. Brodsky, D. S. Hwang and I. Schmidt, Phys. Lett. B **530**, 99 (2002) [hep-ph/0201296].
- [73] L. Gamberg and Z. -B. Kang, Phys. Lett. B **696**, 109 (2011) [arXiv:1009.1936 [hep-ph]].
- [74] K. Kanazawa and Y. Koike, Phys. Rev. D **83**, 114024 (2011) [arXiv:1104.0117 [hep-ph]].
- [75] A. Accardi and J. -W. Qiu, JHEP **0807**, 090 (2008) [arXiv:0805.1496 [hep-ph]].
- [76] A. Accardi and W. Melnitchouk, Phys. Lett. B **670**, 114 (2008) [arXiv:0808.2397 [hep-ph]].
- [77] A. Accardi, T. Hobbs and W. Melnitchouk, JHEP **0911**, 084 (2009) [arXiv:0907.2395 [hep-ph]].
- [78] L. T. Brady, A. Accardi, T. J. Hobbs and W. Melnitchouk, Phys. Rev. D **84**, 074008 (2011) [Erratum-ibid. D **85**, 039902 (2012)] [arXiv:1108.4734 [hep-ph]].
- [79] F. M. Steffens, M. D. Brown, W. Melnitchouk and S. Sanches, arXiv:1210.4398 [hep-ph].